DOI: 10.1002/chem.200500677

Lower Main-Group Element Complexes with a Soft Scorpionate Ligand: The Structural Influence of Stereochemically Active Lone Pairs

Christopher A. Dodds, John Reglinski,* and Mark D. Spicer*[a]

Abstract: The syntheses and structures of complexes of the fifth period elements indium and antimony, and the sixth period element bismuth with the soft scorpionate ligand, hydrotris(methimazolyl)borate (Tm^{Me}) are reported. A considerable variety of structural motifs were obtained by reaction of the main-group element halide and $NaTm^{Me}$. The indium(III) complexes took the form $[In(\kappa^3\text{-}Tm^{Me})_2]^+$. This motif could not, however, be isolated for antimony(III), the dominant product being $[Sb(\kappa^3\text{-}Tm^{Me})(\kappa^1\text{-}Tm^{Me})X]$ (X = Br, I). An iodo-bridged species $[Sb(\kappa^3\text{-}Tm^{Me})I(\mu_2\text{-}I)]_2$, analogous to a previously reported bismuth complex, was also isolated. Reaction of antimony(III) acetate with $NaTm^{Me}$ results in a remarkable species in which three different ligand binding modes are observed. In each antimony complex the influence of the nonbonded electron pair is observed in the structure. Bismuth halides form complexes analogous to those of antimony, with directional lone pairs, but in addition, reaction of $Bi(NO_3)_3$ with $NaTm^{Me}$ results in a complex with a regular S_6 coordination sphere and a nonstereochemically active lone pair. Comparisons are drawn with known Tm^{Me} complexes of As, Sn, and Bi in which the stereochemical influence of the lone pairs is negligible and with Tm^{Me} complexes of Te and Bi in which the lone pairs are stereochemically active. This study highlights the ability of Tm^{Me} to coordinate in a variety of modes as dictated by the metal centre with no adverse effects on the stability of the complexes formed.

Keywords: coordination modes · main group elements · S ligands · scorpionates · tripodal ligands

Introduction

The field of poly(pyrazolyl)borate chemistry has been studied extensively, since the introduction of this ligand system in 1966 by Trofimenko.[1] Over 170 different N-donor scorpionate ligands have now been prepared, with varying degrees of substitution and steric bulk incorporated onto the pyrazolyl rings.[2] These ligands are readily prepared, with hydrotris(pyrazolyl)borate (Tp) and hydrotris(3,5-dimethylpyrazolyl)borate (Tp*) being the most commonly utilized members of this family of ligands. Complexes of poly(pyrazolyl)borates with every d-block element are known and a variety of oxidation states and coordination geometries are supported. These versatile ligands have also found application as key components in materials science,[3] catalysis[4] and coordination chemistry.[5]

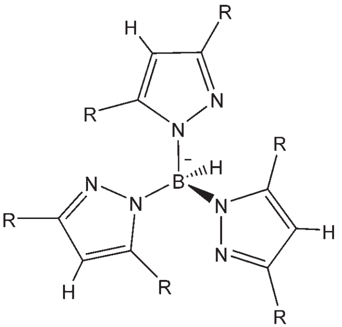

Tp R = H; Tp* R = Me

While the chemistry of poly(pyrazolyl)borates with transition metals has received considerable attention and continues to expand, the chemistry of these ligands with the softer, lower main-group elements is much less developed and remains fragmented. On examination of the literature, it is evident that the boundaries of poly(pyrazolyl)borate chemistry are effectively reached on passing Group 14, although a single structurally characterised bismuth complex has recently been reported.[6] The paucity of stable com-

---

[a] C. A. Dodds, Dr. J. Reglinski, Dr. M. D. Spicer
Department of Pure & Applied Chemistry
University of Strathclyde, 295 Cathedral St.
Glasgow, G1 1XL (UK)
Fax: (+44) 141-552-0876
E-mail: j.reglinski@strath.ac.uk
m.d.spicer@strath.ac.uk

plexes of the remaining lower main-group ions may be regarded as principally due to the hard nature of the ligand and the softness of the elements, and thus a progressive study across the lower main group using poly(pyrazolyl)borates has not been possible thus far.

The recent explosion of interest in soft analogues of Tp, particularly the S_3-donor hydrotris(methimazolyl)borate (Tm^{Me}),[7,8] has allowed stable scorpionate complexes of the lower main group to be synthesized. This soft tripodal ligand readily forms complexes with the heavier group 13–16 elements. Already, well-characterized complexes are known with thallium(I/III),[9,10] tin(IV),[11] arsenic(III),[11] bismuth(III)[12] and tellurium(II),[6] while the bulkier tris(1-phenyl-2-thioimidazolyl)borate (Tm^{Ph}) ligand also supports complexes of lead(II).[13,14] Other soft scorpionate ligands known to form complexes with the lower main-group elements are the hydrotris(thiazolyl)borates (Tz and Tbz) and the unique ambidentate (N_3/S_3 donor) hydrotris(thioxotriazolinyl)borates (Tt). Thallium(I) compounds have been formed with the thiazolyl-based borates,[10] while tin(IV) and bismuth(III) complexes have been generated with the thioxotriazolinyl borates.[15,16]

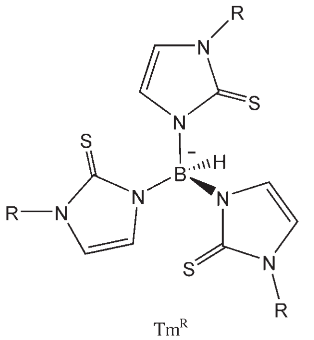

Tm^R

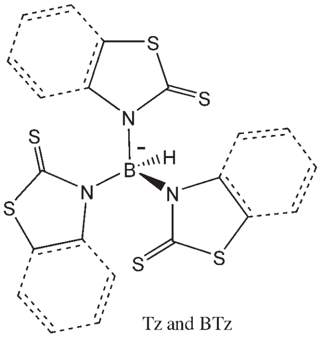

Tz and BTz

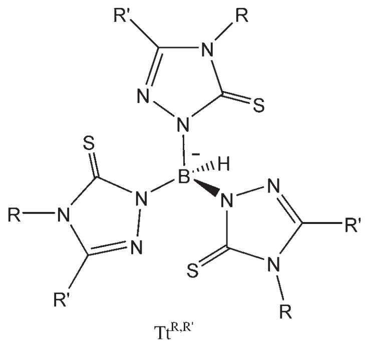

$Tt^{R,R'}$

These complexes display a variety of structural motifs, but the general preference is for the ligand to coordinate in a κ^3 mode. The majority of the complexes formed have a ligand to metal ratio of 2:1, with the dominant motif being a cationic sandwich structure (Scheme 1).

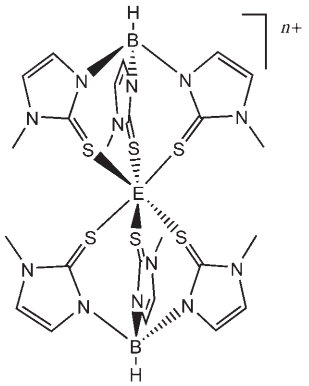

Scheme 1. The cationic sandwich motif adopted by Tm^R ligands with lower main-group elements.

Various other motifs have also been observed in main-group element complexes, with the chemistry of tin(IV) effectively illustrating the ability to control the bonding mode of the ligand by tuning the steric bulk around the metal ion. In the unusual complex $[Sn(Tm^{Me})(Cy)_3]$, the ligand is coordinated in a κ^1 mode due to the presence of three bulky, nonlabile cyclohexyl groups.[17] The chemistry of lead(II) with Tm^{Ph} also displays two structural motifs not observed elsewhere. When the ratio of ligand to metal is 1:1 the simple salt $[Pb(\kappa^3\text{-}Tm^{Ph})][ClO_4]$ is obtained, with the cation assuming a trigonal pyramidal geometry.[13] On increasing the ratio of ligand to metal to 2:1, a second ligand associates with the lead ion. One ligand remains coordinated in the usual κ^3 mode, while the other is only weakly associated with the metal in an inverted configuration, with three thione sulfur atoms and the hydride directed towards the metal.[14] The average Pb–S bond lengths in the secondary ligand are 3.471 Å, compared to 2.848 Å for the κ^3 ligand. The formation of this unusual structure has been attributed to the increased steric bulk in Tm^{Ph}, which prevents the two ligands from coordinating to the metal centre. This argument is not unambiguous, since although a lead complex of the parent ligand Tm^{Me} has been prepared, it has not been structurally characterised,[12] and thus no direct comparison has been possible to quantify the effect of the increased steric bulk.

It is evident that, in contrast to their N-donor congeners, the S-donor tripodal borate ligands are capable of supporting a wide variety of complexes with the lower main-group elements. Herein, we report the preparation and characterisation of antimony and bismuth complexes with Tm^{Me} and undertake the first systematic evaluation across Groups 13–16 with use of the soft scorpionate ligand Tm^{Me}.

Results

We have previously described the preparation of arsenic (III),[11] bismuth(III)[12] and tin(IV)[11] complexes with Tm^{Me} from their respective halides, together with a brief report of a tellurium(II) complex.[6] Extension of this methodology has facilitated the synthesis of the first Tm^{Me} complexes with indium and antimony, together with new complexes of bismuth. In each case a small excess of ligand was added to the appropriate metal halide under broadly similar conditions, ensuring that the structural motif adopted was driven primarily by the identity of the metal, not other experimental factors.

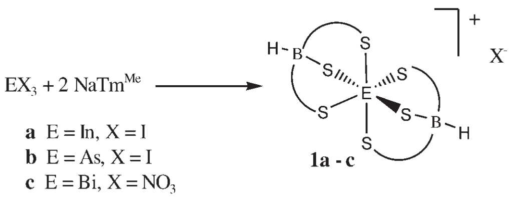

Scheme 2.

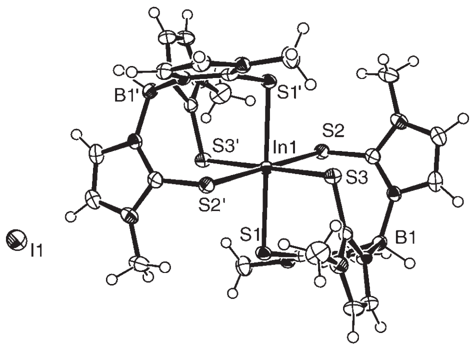

Figure 1. X-ray crystal structure of $[In(\kappa^3\text{-}Tm^{Me})_2]I$ (**1a**) with thermal ellipsoids shown at the 50 % level.

Table 1. Summary of key structural parameters in $[E(Tm^{Me})_2]^{n+}$ complex ions.

	In^{III} [a]	Tl^{III} [b]	Sn^{IV} [c]	As^{III} [c]	Bi^{III} [d]
intra S-E-S [°] [e]	92.35(3) 93.22(3) 93.86(2)	92.2(2) 92.4(2)	92.98(2) 93.10(3) 93.35(3)	92.29(3) 93.54(3) 94.45(3)	89.81(7) 91.31(6) 90.72(6)
inter S-E-S [°]	86.14(2) 86.78(3) 87.65(3)	84.4(2)	86.65(3) 86.90(3) 87.02(3)	85.55(3) 86.46(3) 87.71(3)	90.19(7) 88.69(6) 89.28(6)
E−S [Å]	2.603(8) 2.622(8) 2.623(8)	2.682(7) 2.690(7)	2.549(9) 2.550(9) 2.555(9)	2.570(10) 2.571(10) 2.590(10)	2.806(2) 2.802(2) 2.802(2)
E···B [Å]	4.128	4.26(6)/ 4.17(2)	4.15	4.12	4.26
intra S···S [Å]	3.80	3.87	3.71	3.75	3.99
inter S···S [Å]	3.60	3.72	3.51	3.53	3.94
N-B-N (av) [°]	112.0	112.8	111.1	111.9	111.6

[a] This Work. [b] Ref. 9. [c] Ref. 11. [d] Ref. 12. [e] Bite Angle.

The reaction of indium triiodide with $NaTm^{Me}$ resulted in the isolation of a white solid analysing as $[In(\kappa^3\text{-}Tm^{Me})_2]I$ (**1a**) (Scheme 2). Mass spectrometry confirms the presence of the $[In(Tm^{Me})_2]^+$ ion, while the ^1H NMR spectrum is sharp, indicating minimal ligand exchange on the NMR timescale. X-ray crystallography reveals (Figure 1) that the cation adopts the same "sandwich" structure as observed in the previously reported $[E(Tm^{Me})_2]^{n+}$ species (E = Tl^{III},[9] Sn^{IV},[11] As^{III}[11] and Bi^{III}[12] and the key structural parameters for these complexes are compared in Table 1). It should be noted that the structure of $[In(Tm^{Me})_2]I{\cdot}2\,DMF{\cdot}H_2O$ is crystallographically isomorphous with that of the corresponding arsenic complex. The indium(III) ion resides on a crystallographic inversion centre in an almost regular S_6 octahedral environment (Figure 1), with interligand S-In-S angles in the range 86.14(2)–87.65(3)°, while the average intraligand S-In-S (bite) angles lie between 92.35(3) and 93.86(2)°; this geometry results in a slight compression of the coordination octahedron, as previously observed[9,11]. There is little variation in the In−S bond lengths (2.6028(8), 2.6219(8) and 2.6231(8) Å), which are comparable with those in the simple octahedral tris-dithiocarbamate complexes of indium(III),[18] but shorter than in the corresponding heavier congener $[Tl(Tm^{Me})_2]^+$ (2.686 Å),[9] by an amount commensurate with the difference in ionic radii of the two ions (Table 1). As expected, the environment around the indium ion is more regular for Tm^{Me} than is seen in dithiocarbamate and related didentate thione donors.

Although Reger et al. have prepared Tp, pzTp and Tp* complexes of indium,[19] no direct analogues of our complex have been observed. Instead, with Tp* a 1:1 adduct $[In(Tp^*)Cl_2]$ is isolated, while with pzTp 2:1 adducts $[In(pzTp)_2Cl]$ and 3:1 adducts $[In(pzTp)_3]$ are obtained. In the 2:1 complexes, the halide is coordinated forcing one ligand to coordinate in a κ^2 mode. However, dissolution in halogenated solvents apparently results in displacement of the chloride ion, thus allowing both ligands to adopt a κ^3 coordination mode. With Tp* the $[In(Tp^*)_2X]$ species is not obtained, possibly due to the steric interactions of the bulkier 3,5-disubstituted ligand.

The reaction of antimony tribromide or triiodide (Scheme 3) with two equivalents of $NaTm^{Me}$ gave rise to yellow–orange crystalline materials that analysed as $[Sb(Tm^{Me})_2]X$ (**2a**,**c**: X = Br, I, respectively). In each case ^1H NMR spectra revealed very broad singlets for the protons on the heterocyclic rings and for the methyl protons, indicative of significant fluxionality in solution. All previous examples of the expected bis-κ^3-Tm^{Me} motif gave well-resolved NMR spectra and the large linewidths observed here suggested to us that this motif had not formed. Mass spectrometry showed the presence of an ion with mass equiva-

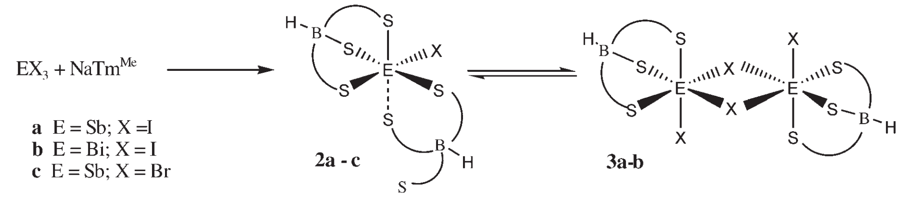

Scheme 3.

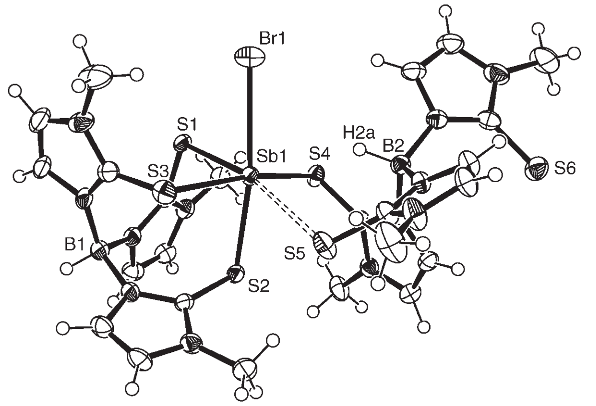

Figure 2. X-ray crystal structure of [Sb(κ^3-Tm^{Me})(κ^1-Tm^{Me})I] (**2c**) with thermal ellipsoids shown at the 50% level.

lent to $[Sb(Tm^{Me})_2]^+$, but X-ray diffraction studies of the isostructural bromide and iodide complexes revealed a "5+1" coordination geometry at the antimony atom, consisting of one Tm^{Me} ligand coordinated in the usual κ^3 mode, one ligand in a κ^1 mode and a halide ion, generating a square-pyramidal primary coordination geometry. The sixth coordination site interacts weakly with a second sulfur atom of the κ^1-coordinated Tm^{Me} ligand. The structure of the bromide is shown in Figure 2 and the key bond lengths and angles are presented in Table 2.

The Sb–S bond lengths for the κ^3-coordinated ligand are in the range 2.55–2.73 Å, while the second ligand has one Sb–S bond length of 2.71 Å, with the second sulfur atom weakly interacting at a distance of approximately 3.26 Å. In addition, the hydride attached to the boron atom approaches the antimony atom (at a distance of 2.87 Å). The Sb–S distances are comparable with those in dithiocarbamate,[20,21] dithiolene[22] and thiophosphonate[23] complexes. Inspection of the Cambridge Crystallographic database[24] reveals that crystallographically determined Sb–S distances lie in the range 2.29–3.49 Å, but with a mean of 2.56 Å and only 4.4% being greater than 3.0 Å. Thus the shortest Sb–S distances in our complexes are generally a little longer than on average, while the longest is quite unusually so. The coordinated halides are also found to have Sb–X bond lengths (2.9163(5) Å (Br) and 3.1498(6) Å (I)) somewhat longer than the average (2.73 Å (Br); 3.05 Å (I)). A significant deviation from ideal octahedral geometry is evident when the bond angles are scrutinized. While the intraligand S-Sb-S bond angles within the κ^3-coordinated ligand are all approximately ideal (between 88 and 90 °), the remainder of the coordination sphere is markedly distorted, with S-Sb-S and I-Sb-S bond angles in the range 74.26–95.18°, indicative of the presence of a stereochemically active lone pair in the vicinity of the weakest Sb–S interaction.

Table 2. Selected bond lengths [Å] and angles [°] for the antimony complexes.

	2c X=Br	**2a** X=I	**3a**	**4**
κ^3 ligand				
Sb–S1	2.5497(9)	2.5578(14)	2.5572(10)	2.6170(8)
Sb–S2	2.6308(10)	2.6177(14)	2.5932(9)	2.6137(8)
Sb–S3	2.7317(10)	2.7249(14)	2.6073(10)	2.5406(8)
κ^1/κ^2 ligand				
Sb–S4	2.7033(10)	2.7135(13)	–	2.9012(9)
Sb–S5	3.3069(11)	3.263	–	2.9183(8)
Sb–X_t	2.9163(5)	3.1498(6)	3.1851(4)	–
Sb–X_{br}	–	–	3.2518(4)	–
Sb···X	–	–	3.3502(4)	–
Sb···H	2.803	2.872	–	3.495
intraligand angles				
S1-Sb-S2	89.34(3)	89.60(4)	90.11(3)	88.98(2)
S1-Sb-S3	88.08(3)	88.35(5)	91.80(3)	91.98(3)
S2-Sb-S3	89.11(3)	89.17(4)	91.77(3)	91.14(3)
S4-Sb-S5	101.88(3)	102.01(6)	–	103.98(2)
interligand angles				
S1-Sb-S4	84.88(3)	84.41(4)	–	90.01(2)
S1-Sb-S5	167.30(3)	167.75(6)	–	163.62(3)
S1-Sb-X	73.71(3)	74.26(3)	73.67(2), 2.96(2), 164.66(2)	–
S2-Sb-S4	79.91(3)	79.66(4)	–	163.96(3)
S2-Sb-S5	81.39(3)	81.42(6)	–	75.21(2)
S2-Sb-X	162.33(3)	163.52(3)	162.55(2), 74.10(2), 89.76(2)	–
S3-Sb-S4	167.00(3)	166.70(5)	–	72.89(3)
S3-Sb-S5	83.14(3)	83.23(6)	–	84.23(3)
S3-Sb-X	95.13(3)	93.56(3)	95.02(2), 165.12(2), 72.91(2)	–
S4-Sb-X	101.89(5)	95.18(3)	–	–
S5-Sb-X	116.10(2)	115.03(7)	–	–

The observed structure prompted us to consider variable-temperature NMR measurements to further probe the dynamic processes in solution. While the iodide complex was poorly soluble in all solvents except DMSO and DMF, thus precluding such measurements, the analogous bromide complex was appreciably more soluble in CH_2Cl_2, allowing observation of ^{1}H NMR spectra in the temperature range 298–218 K. At the lower temperature the resonances began to broaden once more, probably indicative of precipitation from solution. The spectra of the methimazole ring protons are shown in Figure 3. It would appear that at least two distinct processes are in operation. Above 298 K a single set of broad resonances is observed, which implies that all the methimazole environments on both Tm^{Me} ligands are equivalent. On cooling, the peaks begin to sharpen, and at 298 K a pair of peaks at $\delta = 6.95$ and 7.02 ppm begin to resolve. These are typical κ^3-coordinated ligands and probably result from the slowing (on the NMR timescale) of the dissociation of the κ^3-coordinated ligand. The spectrum continues to sharpen until 258 K, at which temperature a further splitting occurs and a pair of sharper peaks and a broad singlet in a 1:2 ratio emerge. This presumably results from slowing the dissociation of the κ^2-coordinated ligand from the central antimony atom. Whereas at higher temperatures all three methimazole environments interconvert, below 258 K the ligand dissociation is slowed to give a sharp resonance for the uncoordinated methimazole. The broad singlet corresponds to the two coordinated methimazole moieties, which apparently still undergo some fluxional process. This may be a dissociative process or possibly a "windscreen-wiper" twist of the two methimazole rings. Hill has observed fluxionality in molybdenum complexes of Tm^{Me}[25] that he ascribes primarily to dissociative processes, but in this case it is not possible to distinguish between the two possibilities.

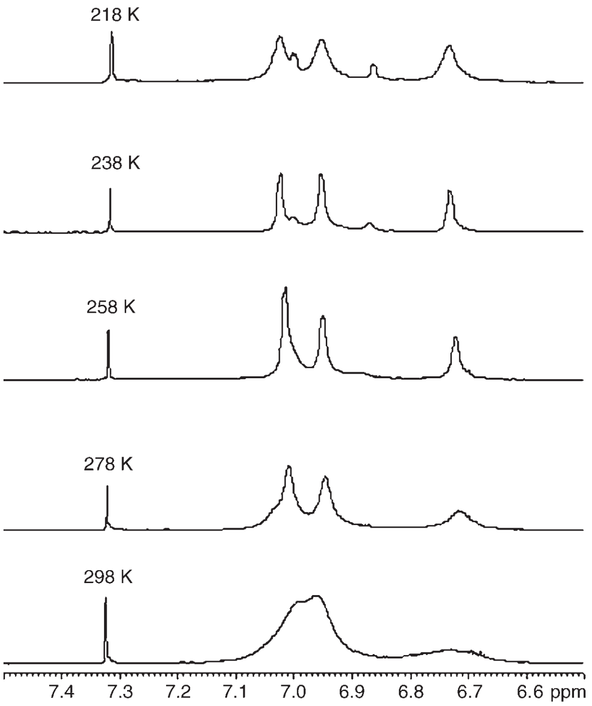

Figure 3. Variable-temperature ^{1}H NMR spectrum of [Sb(κ^3-Tm^{Me})(κ^1-Tm^{Me})Br] (**2c**) in the temperature range 298–218 K.

On occasion, a second crystalline material (yellow needles as opposed to orange blocks) was obtained from the reaction of SbI$_3$ with NaTm^{Me}; X-ray diffraction revealed these crystals to be a dimeric complex, [{Sb(Tm^{Me})I(μ_2-I)}$_2$] (**3a**: Scheme 3, Figure 4), analogous to that of the corresponding bismuth complex, [{Bi(Tm^{Me})Cl(μ_2-Cl)}$_2$].[12] The dimer is disposed about a crystallographic centre of symmetry with the geometry around the antimony(III) ion being distorted octahedral. The Tm^{Me} ligands are coordinated in the κ^3 mode and are highly regular. The Sb–S bond lengths range from 2.56–2.61 Å, showing less variation than in the mononuclear halo complexes described above. The S-Sb-S bond angles range from 90.1–95.0°, which are comparable to the intraligand S-E-S bond angles observed in the lower main-group complexes [E(Tm^{Me})$_2$]$^{n+}$ (E = As, Tl, Bi $n=1$; E = Sn, $n=2$) . The terminal iodide has an Sb–I bond length of 3.1851(4) Å, again somewhat longer than the average of crystallographically determined Sb–I distances (3.05 Å). The iodide bridge is asymmetric with one Sb–I bond length significantly shorter (3.2518(4) Å) than the other (3.3502(4) Å), similar to distances previously observed in [{Sb(RR'dtc)$_2$(μ_2-I)}$_2$] (3.280 and 3.359 Å).[21] The presence of stereochemically active lone pairs on the antimony(III) ions is again clear, as evidenced by the I-Sb-I bond angles, which are all substantially larger than expected for ideal octahedral geometry, with values of 99.852(10), 101.74(10) and 107.594(10)°. In this case the lone pair apparently occupies one face of the coordination octahedron.

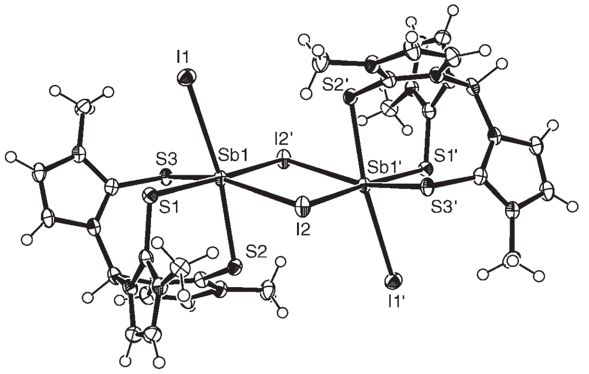

Figure 4. X-ray crystal structure of [{Sb(κ^3-Tm^{Me})(μ_2-I)I}$_2$] (**3a**) with thermal ellipsoids shown at the 50% level.

It should also be noted that this species does not appear to be representative of the bulk material obtained from these reactions. Microanalysis and mass spectral data are all identical to and consistent with the monomeric halide species described above. It would seem that the dimer is in equilibrium with [Sb(κ^3-Tm^{Me})(κ^1-Tm^{Me})I] (**2a**) and is able to form at low concentrations in solution in the presence of excess halide and crystallises preferentially. It is interesting to note that the known bismuth analogue [{Bi(Tm^{Me})Cl(μ_2-Cl)}$_2$] was also isolated in similar circumstances.[12]

Since halide was present in the coordination sphere of each of the species obtained, a halide-free precursor was sought in an effort to prepare the S_6-donor $[Sb(\kappa^3\text{-}Tm^{Me})_2]^+$ ion. Reaction of $Sb(OAc)_3$ with $NaTm^{Me}$ in methanol (Scheme 4) resulted in the formation of a yellow solid (**4**), the mass spectrum of which contained a species with the appropriate *m*/*z*. However, the proton NMR spectrum was once again extremely broad, indicating significant fluxionality and suggesting that the desired species was again not obtained. The IR spectrum showed two ν_{B-H} frequencies, one at $2450\,cm^{-1}$ corresponding to a coordinated Tm^{Me} ligand and one at $2510\,cm^{-1}$ indicative of free Tm^{Me}. Once more, crystallography revealed the true nature of this species (Figure 5). The antimony centre has a primary coordination sphere that contains five sulfur donor atoms in a square-pyramidal arrangement. One Tm^{Me} ligand is coordinated in the usual tridentate κ^3 mode with Sb–S distances in the range 2.54–2.62 Å, while a second is in an "inverted" bidentate κ^2 mode reminiscent of the conformation adopted by one of the ligands in $[Te(\kappa^2\text{-}Tm^{Me})_2]$.[6] In the present case the Sb–S bond distances are much longer at 2.901 and 2.918 Å. The third Tm^{Me} anion is weakly associated with the complex in the vicinity of the vacant coordination site. It is interesting to note that in solution at room temperature the coordinated and non-coordinated Tm^{Me} species exchange with one another, as evidenced by a single set of methimazole resonances in the ^1H NMR spectrum. This is in contrast to the situation observed in $[Sn(Tm^{Me})_2][Tm^{Me}]_2$,[11] in which sharp peaks for both the coordinated and free Tm^{Me} anions are observed. Again the influence of the stereochemically active lone pair is evident from the distortion of the primary coordination polyhedron.

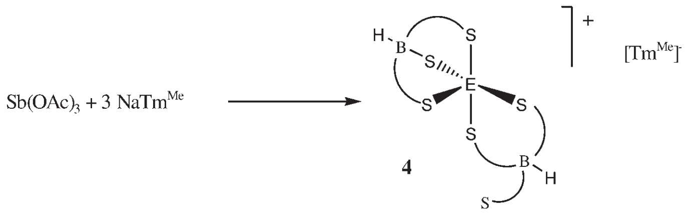

Scheme 4.

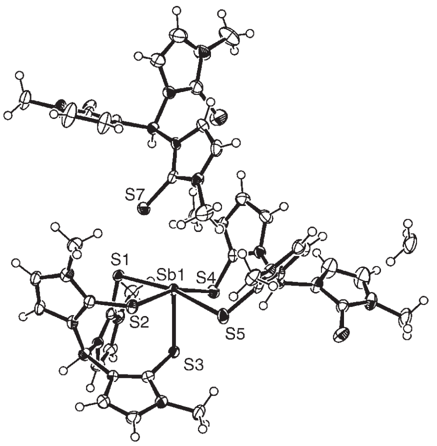

Figure 5. X-ray crystal structure of $[Sb(\kappa^3\text{-}Tm^{Me})(\kappa^2\text{-}Tm^{Me})]Tm^{Me}$ (**4**) with thermal ellipsoids shown at the 50 % level.

Our previous studies on bismuth Tm^{Me} complexes[12] revealed a chloro-bridged dimer analogous to the dimeric antimony complex reported here; this bismuth dimer showed clear signs of distortion of the coordination sphere due to the lone pair. Recently, Shimada[26] has also reported a similar complex, $[\{Bi(Tm^{tBu})Cl(\mu_2\text{-}Cl)\}_2]$, formed from the Tm^{tBu} ligand and $BiCl_3$. In addition, we have been able to prepare a regular octahedral complex, $[Bi(Tm^{Me})_2]^+$, in which the lone pair showed no structural influence.[12] Finally, a complex which analyses as $[Bi(Tm^{Me})_2Cl]$ has been prepared in our laboratories, but has not been fully characterised. In the light of our studies with the lighter Group 15 elements, it was decided to reinvestigate the reaction of bismuth halide with $NaTm^{Me}$. Reaction of BiI_3 with $NaTm^{Me}$ (Scheme 3) resulted in the formation of an orange solid (**2b**). The mass spectrum of this species showed only the presence of $[Bi(Tm^{Me})_2]^+$, but the ^1H NMR spectrum was very broad, inconsistent with the regular octahedral $[E(Tm^{Me})_2]^{n+}$ complexes. The X-ray crystal structure[27a] showed the compound to be isomorphous with the monomeric species **2a**,**c** described above. Since the previously reported example of a regular octahedral complex, $[Bi(Tm^{Me})_2]^+$, had been prepared by an indirect route, we decided to investigate whether such a species could also be prepared directly from a halide-free precursor. Reaction of $Bi(NO_3)_3$ with $NaTm^{Me}$ resulted in the formation of a burgundy solid (**1c**), which gave a sharp ^1H NMR spectrum and the crystal structure[27b] of which revealed the expected regular S_6 donor set (Scheme 2). Thus there is a divergence in the behaviour of bismuth from that of antimony, in that the former is able, in favorable circumstances, to adopt a regular S_6 donor set, while the latter seems unwilling to do so.

Discussion

A significant body of structural data is now available for a series of Tm^{Me} complexes across the fifth period (In–Te) and also down Group 15 (As–Bi) and a comparison of the structures adopted is instructive. Interestingly a variety of structural motifs are observed, with the ligand demonstrating considerable flexibility, coordinating not only in the κ^3 mode as expected but also in κ^1 and κ^2 modes and, unlike the Tp anion,[28] readily acting as a non-coordinating anion.

Traversing period 5 a gradation of structures is observed. Both In^{III} and Sn^{IV}, which do not have non-bonded electron pairs, adopt close to regular octahedral coordination geometries with bond lengths spanning small ranges (±0.020 Å for In and ±0.006 Å for Sn). On moving to antimony(III), a single lone pair is present in each complex, and without exception the lone pair is stereochemically active. This leads to a "5+1" coordination geometry in which the primary coordination sphere is approximately square pyramidal. Finally, the previously reported tellurium(II) complex,[6] with two lone pairs, adopts the square-planar structure predicted by VSEPR theory.

It is interesting to note, however, that on descending Group 15 the behaviour observed does not follow an intuitively obvious trend. The trivalent cations all formally have a non-bonded electron pair, but the As^{III} complex unexpectedly adopts a regular octahedral geometry. The Sb^{III} complexes, as discussed above, form either square-pyramidal or highly distorted octahedral structures, consistent in every case with stereochemically active lone pairs. Finally, Bi^{III} is able to adopt both types of structure. In the presence of halide, the structures have stereochemically active lone pairs, but in the absence of halide regular octahedral S_6 coordination is observed.

There are remarkably few homologous series of complexes of this type. One example, in which a similar structural progression has been observed, was recently reported by Levason et al. They prepared As, Sb and Bi complexes of a cyclic diselenoether ligand, 1,5-diselenacyclooctane ([8]aneSe$_2$),[29] of the form $[E_2Cl_6(\mu\text{-}[8]aneSe_2)_2]$ (E = As, Sb,Bi) in which the E_2Cl_6 units were planar halide-bridged dimers linked into polymeric arrays by means of bridging macrocyclic ligands. In the case of the As and Bi species the links were symmetric, indicating no significant lone-pair interactions, while the Sb species showed a very marked asymmetry (Scheme 5). These observations run counter to the situation most commonly observed, such as in the compounds EI_3 (E = As, Sb, Bi). The Group 15 element is situated in an octahedral lattice site, and in the case of bismuth, the Bi–I interactions result in a regular octahedral geometry. Antimony and arsenic, however, show an increasing disparity between the so-called primary and secondary interactions[30] resulting in three short and three longer E–I bonds, thus giving very distorted coordination spheres. In general, the observed differences between primary and secondary bonding are in the order As > Sb > Bi.[31]

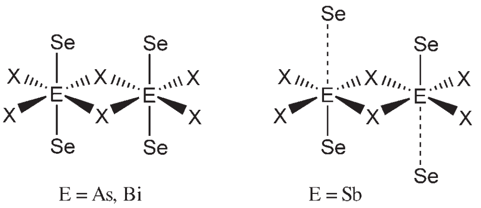

Scheme 5. The coordination spheres of $[E_2Cl_6([8]aneSe_2)_2]$ (E = As, Sb, Bi).

It is widely accepted[32] that when the lone pair occupies an s orbital, the effect is to give regular geometry and slightly lengthen all of the E–L distances, whereas when the lone pair occupies a p-orbital (or some hybrid thereof) then the effect it is more directional in nature. What is less clear is which factors drive a system towards one extreme or the other. In that they all adopt structures with stereochemically active lone pairs, the antimony complexes reported behave in the manner predicted by classical theories. Furthermore, the bismuth structures are presumably influenced by relativistic effects, which lower the energy of the 6s orbital[33] (the inert pair effect), which in turn results in a greater propensity to non-directional lone pairs. Thus, a regular S_6 coordination sphere is attainable. However, in the presence of halide ions the energy balance is sufficiently shifted to allow a directional lone pair to be observed. In the cases in which the lone pair is stereochemically active, the complexes broadly adopt the characteristics described by Hancock,[34] in that the bond mutually *trans* to the believed site of the lone pair is shortest, while as the angle from a bond to the lone pair decreases, the element to donor atom bond length increases.

The case of arsenic remains problematic, as it would be expected that $[As(Tm^{Me})_2]^+$ would present the most distorted structure, but it is in fact highly regular. Most species with AsS_6 coordination show distinct primary and secondary bonding, with three short As–S distances and three longer, mutually *trans* As–S distances (Scheme 6a). For example: $As(S_2COiPr)_3$ 2.305/2.978 Å,[35] $As(S_2P\{OMe\}_2)_3$ 2.315/3.031 Å,[36] $As(S_2CNnBu_2)_3$ 2.347/2.875 Å[37] and $As(S_2C\text{-}p\text{-}tol)_3$ 2.317/2.969 Å.[38] The only previously reported example of an essentially regular AsS_6 species occurs when two $\{Mo_3(\mu_3\text{-}S)(\mu_2\text{-}S)_3(OH_2)_9\}$ clusters "sandwich" an As^{3+} ion, coordinating by means of the di-bridging sulphides, giving As–S bond lengths in the narrow range 2.434–2.489 Å (Scheme 6b).[39] A similar lack of distortion has already been noted in Levason's seleno–ether macrocycle complex.[29] The factors which result in a stereochemically inactive lone pair in these cases are not clear and will be the subject of future investigations.

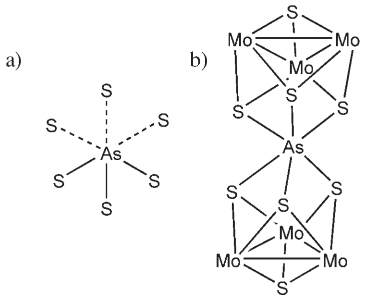

Scheme 6. a) Representation of the primary and secondary coordination commonly seen in AsS_6 coordination polyhedra. b) The core structure of the only previously reported species having a regular AsS_6 coordination sphere, $[As(Mo_3(\mu_3\text{-}S)(\mu_2\text{-}S)_3(OH_2)_9)]^{8+}$. Note that each molybdenum atom is also ligated by three water molecules.

Experimental Section

General considerations: $NaTm^{Me}$ was prepared by literature methods.[8] All other reagents were obtained commercially and used as supplied. The complexes prepared were stable to air and moisture and inert atmospheres were not used in their preparations. NMR spectra were recorded on a Bruker DPX400 spectrometer operating at 400 MHz for ^{1}H and 100 MHz for ^{13}C. The ^{1}H and ^{13}C spectra were referenced by using internal solvent peaks to TMS. IR spectra were recorded as KBr discs on a Nicolet Avatar 360 FT-IR spectrometer. Mass spectrometry was carried out by the EPSRC service using a Voyager-DE-STR spectrometer.

Synthesis of [In(κ^3-Tm^{Me})$_2$]I (1a): Indium(III) iodide (0.182 g, 0.37 mmol) was dissolved in chloroform (15 mL) and NaTm^{Me} (0.277 g, 0.74 mmol) was added. The mixture was stirred for 24 h and the resulting white solid was filtered off. The crude solid was suspended in water and stirred. Complex **1a** was isolated by filtration, was washed with methanol (2× 15 mL) and diethyl ether (20 mL), and was dried in air. Yield: 148 mg, 42%. Colourless crystals suitable for X-ray diffraction were obtained by vapour diffusion of diethyl ether into a solution of **1a** in DMF. Elemental analysis calcd (%) for $C_{24}H_{32}N_{12}S_6B_2InI$: C 30.6, H 3.4, N 17.8; found: C 30.8, H 3.5, N 17.3; ^{1}H NMR ([D$_6$]DMSO): $\delta = 3.51$ (s, 3H; -CH$_3$), 7.17 (d, 1H; -CH), 7.45 ppm (d, 1H; -CH); IR (KBr disc): $\tilde{\nu} = 2433$ cm^{-1} (B–H); MS (MALDI): m/z (%): 817 (100) [M]$^+$.

Synthesis of [Sb(κ^3-Tm^{Me})(κ^1-Tm^{Me})I] (2a): NaTm^{Me} (0.327 g, 0.87 mmol) was suspended in acetone (15 mL), antimony(III) iodide (0.217 g, 0.43 mmol) dissolved in acetone (15 mL) was added and the mixture was stirred for 3 h. The resulting yellow solid was filtered off and extracted with DMF. The orange solution was filtered through Celite and the product isolated as orange crystals by vapor diffusion with diethyl ether. Yield: 0.245 g, 60%; elemental analysis calcd (%) for $C_{24}H_{32}N_{12}S_6B_2SbI$: C 30.3, H 3.4, N 17.7; found: C 30.3, H 3.6, N 17.2; ^{1}H NMR ([D$_6$]DMSO): $\delta = 3.62$ (s, 3H; -CH$_3$), 7.12 (br s, 1H; -CH), 7.43 ppm (br s, 1H; -CH); IR (KBr disc): $\tilde{\nu} = 2453$ cm^{-1} (B–H); MS (MALDI): m/z (%): 823 (76) [M–I]$^+$.

Synthesis of [Bi(κ^3-Tm^{Me})(κ^1-Tm^{Me})I] (2b): The analogous bismuth iodide complex was prepared in the same way from BiI$_3$ (0.254 g, 0.43 mmol) and NaTm^{Me} (0.337 g, 0.90 mmol). Yield: 0.370 g, 79%; elemental analysis calcd (%) for $C_{24}H_{32}B_2BiIN_{12}S_6 \cdot 0.75\,DMF$: C 28.8, H 3.4, N 16.3; found: C 29.0, H 3.2, N 16.0; ^{1}H NMR ([D$_6$]acetone): $\delta = 3.62$ (br s, 3H), 3.86 (br s, 3H), 6.93 (br s, 1H), 7.03 (br s, 1H), 7.24 (br s, 1H), 7.40 ppm (br s, 1H); IR (KBr disc): $\tilde{\nu} = 2428$, 2402 cm^{-1} (B–H); MS (MALDI): m/z: 911.0 [M–I]$^+$.

Synthesis of [Sb(κ^3-Tm^{Me})(κ^1-Tm^{Me})Br] (2c): The analogous antimony bromide complex was prepared similarly from SbBr$_3$ (0.180 g, 0.50 mmol) and NaTm^{Me} (0.40 g, 1.07 mmol). Yield: 0.322 g, 71%. The crude solid was redissolved in CHCl$_3$, filtered through Celite and taken to dryness in vacuo. Elemental analysis calcd (%) for $C_{24}H_{32}B_2BrN_{12}S_6Sb \cdot 1.25\,CHCl_3$: C 28.8, H 3.2, N 16.0; found: C 28.8, H 2.9, N 15.7; ^{1}H NMR ([D$_6$]DMSO): $\delta = 3.51$ (br s, 3H), 3.75 (br s, 3H), 6.95 (br s 1H), 7.07 (br s, 1H), 7.23 (br s, 1H), 7.53 ppm (br s, 1H); IR (KBr disc): $\tilde{\nu} = 2454$ cm^{-1} (B–H); MS (MALDI): m/z: 825.0 [M–Br]$^+$.

Synthesis of [Sb(κ^3-Tm^{Me})(κ^2-Tm^{Me})][Tm^{Me}] (4): Sb(OAc)$_3$ (0.15 g, 0.5 mmol) was dissolved in methanol (10 mL) and added to a solution of NaTm^{Me} (0.4 g, 1.07 mmol) in methanol (15 mL). The initially colourless solution turned deep red, and over a period of approximately 2 h a yellow solid precipitated. This was collected by filtration, was washed with diethyl ether and was dried in vacuo. Yield: 0.334 g, 80%. The product could be further purified by vapour diffusion of Et$_2$O into a solution of **4** in CHCl$_3$. X-ray quality crystals were obtained by allowing solutions of Sb(OAc)$_3$ and NaTm^{Me} in methanol to slowly diffuse into one another through a methanol blank over a period of one month. Elemental analysis calcd (%) for $C_{36}H_{48}B_3N_{18}S_9Sb \cdot 2\,CHCl_3$: C 32.3, H 3.6, N 17.8; found: C 32.2, H 3.5, N 18.5; ^{1}H NMR ([D$_6$]DMSO): $\delta = 3.31/3.52$ (v br, 6H), 6.58 (v br, 1H), 6.92 (v br, 1H), 7.12 (br s, 1H), 7.45 ppm (br s, 1H); IR (KBr disc): $\tilde{\nu} = 2443$, 2510 cm^{-1} (B–H); MS (MALDI): m/z (%): 823 (100) [Sb(Tm^{Me})$_2$]$^+$.

Synthesis of [Bi(Tm^{Me})$_2$]NO$_3$ (1c): Bi(NO$_3$)$_3$·5 H$_2$O (0.29 g, 0.60 mmol) suspended in acetone (10 mL) was added to NaTm^{Me} (0.4 g, 1.07 mmol) in acetone (10 mL). A deep red/purple colour formed immediately and after stirring for 24 h a purple solid had separated. This was collected by filtration. The crude material was redissolved in CHCl$_3$, was filtered through Celite and was taken to dryness in vacuo. Yield: 0.451 g, 87%; elemental analysis calcd (%) for $C_{24}H_{32}B_2BiN_{13}O_3S_6 \cdot 1.5\,CHCl_3$: C 26.6, H 2.9, N 15.8; found: C 26.3, H 2.8, N 15.6; ^{1}H NMR (CDCl$_3$): $\delta = 3.71$ (s, 3H), 6.85 (s, 1H), 6.97 ppm (s, 1H); IR (KBr disc): $\tilde{\nu} = 2428$ cm^{-1} (B–H).

X-ray crystallography: Crystals were coated in mineral oil and mounted on glass fibres. Data were collected at 123 K on a Nonius Kappa CCD diffractometer by using graphite-monochromated Mo$_{K\alpha}$ radiation. The heavy atom positions were determined by Patterson methods and the remaining atoms located in difference electron density maps. Full-matrix least-squares refinement was based on F^2, with all non-hydrogen atoms anisotropic. While hydrogen atoms were mostly observed in the difference maps, they were placed in calculated positions riding on the parent atoms. In several of the structures there were solvent molecules that were only partially present or were severely disordered, resulting in less than ideal crystallographic parameters.[27] The structure solution and refinement used the program SHELX-97[40] and the graphical interface WinGX.[41] A summary of the crystallographic parameters is given in Table 3. CCDC-274853–274859 contains the supplementary crystallo-

Table 3. Crystallographic parameters.

	1a	**2a**	**2c**	**3a**	**4**
formula	$C_{34}H_{55}B_2IInN_{14}O_3S_6$	$C_{28.5}H_{44.5}B_2IN_{13.5}O_{2.5}S_6Sb$	$C_{28.5}H_{44.5}B_2BrN_{13.5}O_{2.5}S_6Sb$	$C_{24}H_{32}B_2I_4N_{12}S_6Sb_2$	$C_{36}H_{48}B_3N_{18}S_9Sb$
M_r	1164.63	1078.56	1031.91	1453.69	1175.64
T [K]	173(2)	173(2)	123(2)	120(2)	123(2)
crystal system	monoclinic	monoclinic	monoclinic	monoclinic	triclinic
space group	$C2/c$	$P2_1/c$	$P2_1/c$	$P2_1/n$	$P\bar{1}$
a [Å]	29.5569(6)	13.8763(2)	13.8587(3)	11.2578(3)	10.5769(3)
b [Å]	17.6791(4)	18.4573(3)	18.3796(4)	16.9970(5)	15.4084(5)
c [Å]	9.9651(3)	18.8110(4)	18.8351(4)	11.6125(3)	19.5119(6)
α [°]	90	90	90	90	75.5330(10)
β [°]	107.6410(10)	94.2250(10)	93.8220(10)	100.8520(10)	79.049(2)
γ [°]	90	90	90	90	73.778(2)
Z	4	4	4	2	4
V [Å^3]	4962.3(2)	4804.76(15)	4786.96(18)	2182.30(10)	2931.69(16)
μ [mm^{-1}]	1.400	1.518	1.715	4.390	0.830
$F(000)$	2354	2160	2088	1360	1200
crystal size [mm]	0.3×0.3×0.2	0.70×0.60×0.30	0.6×0.6×0.1	0.28×0.15×0.12	0.30×0.20×0.05
reflns measd	28 922	21 303	20 689	13 199	24 887
unique reflns	5697 ($R_{int} = 0.0595$)	11 006 ($R_{int} = 0.0386$)	10 873 ($R_{int} = 0.0288$)	4989 ($R_{int} = 0.0345$)	13 344 ($R_{int} = 0.0359$)
parameters	298	532	525	229	601
R[a] [$I > 2\sigma(I)$]	0.0369	0.0507	0.0433	0.0284	0.0429
wR[b] (all data)	0.0934	0.1726	0.1322	0.0689	0.1426
GOF	1.023	1.076	0.944	0.889	0.588

[a] $R = \Sigma||F_o|-|F_c||/\Sigma|F_o|$. [b] $wR = \{\Sigma[w(F_o^2-F_c^2)^2]/\Sigma[w(F_o^2)^2]\}^{1/2}$.

graphic data for this paper. These data can be obtained free of charge from The Cambridge Crystallographic Data Centre via www.ccdc.cam.ac.uk/data_request/cif.

Acknowledgements

We thank the EPSRC for funding (C.A.D.) and the EPSRC National Mass Spectrometry Service Centre, University of Wales, Swansea for mass spectrometric measurements.

---

[1] S. Trofimenko, *J. Am. Chem. Soc.* **1966**, *88*, 1842–1844.
[2] S. Trofimenko, *Scorpionates: The Coordination Chemistry of Polypyrazolylborate Ligands*, Imperial College Press, London, **1999**.
[3] B. S. Harrison, T. J. Foley, A. S. Knefely, J. K. Mwaura, G. B. Cunningham, T.-S. Kang, M. Bouguettaya, J. M. Boncela, J. R. Reynolds, K. S. Schanze, *Chem. Mater.* **2004**, *16*, 2938–2947.
[4] L. L. Blosch, K. Abboud, J. M. Boncella, *J. Am. Chem. Soc.* **1991**, *113*, 7066–7068.
[5] "Scorpionate and Related Ligands" *Polyhedron* **2004**, *23*, 195–508.
[6] C. A. Dodds, A. R. Kennedy, J. Reglinski, M. D. Spicer, *Inorg. Chem.* **2004**, *43*, 394–395.
[7] M. Garner, J. Reglinski, I. Cassidy, M. D. Spicer, A. R. Kennedy, *Chem. Commun.* **1996**, 1975–1976.
[8] J. Reglinski, M. Garner, I. D. Cassidy, P. A. Slavin, M. D. Spicer, D. R. Armstrong, *J. Chem. Soc. Dalton Trans.* **1999**, 2119–2126.
[9] P. A. Slavin, J. Reglinski, M. D. Spicer, A. R. Kennedy, *J. Chem. Soc. Dalton Trans.* **2000**, 239–240.
[10] J. F. Ojo, P. A. Slavin, J. Reglinski, M. Garner, M. D. Spicer, A. R. Kennedy, S. J. Teat, *Inorg. Chim. Acta* **2001**, *313*, 15–20.
[11] C. A. Dodds, M. Jagoda, J. Reglinski, M. D. Spicer, *Polyhedron* **2004**, *23*, 445–450.
[12] J. Reglinski, M. D. Spicer, M. Garner, A. R. Kennedy, *J. Am. Chem. Soc.* **1999**, *121*, 2317–2318.
[13] B. M. Bridgewater, G. Parkin, *J. Am. Chem. Soc.* **2000**, *122*, 7140–7141.
[14] B. M. Bridgewater, G. Parkin, *Inorg. Chem. Commun.* **2000**, *3*, 534–536.
[15] P. J. Bailey, M. Lanfranchi, L. Marchio, S. Parsons, *Inorg. Chem.* **2001**, *40*, 5030–5035.
[16] M. Careri, L. Elviri, M. Lanfranchi, L. Marchio, C. Mora, M. A. Pellinghelli, *Inorg. Chem.* **2003**, *42*, 2109–2114.
[17] C. Santini, M. Pellei, G. Gioia Lobbia, C. Pettinari, A. Drozdov, S. Troyanov, *Inorg. Chim. Acta* **2001**, *325*, 20–28.
[18] K. Dymock, G. J. Palenik, J. Slezak, C. L. Raston, A. H. White, *J. Chem. Soc. Dalton Trans.* **1976**, 28–32.
[19] D. L. Reger, S. S. Mason, A. L. Rheingold, R. L. Ostrander, *Inorg. Chem.* **1994**, *33*, 1803–1810.
[20] V. Venkatachalem, K. Ramalingam, U. Casellato, R. Grazianic, *Polyhedron* **1997**, *16*, 1211–1221.
[21] V. Venkatachalam, K. Ramalingam, G. Bocelli, A. Cantoni, *Inorg. Chim. Acta* **1997**, *261*, 23–28.
[22] N. Avarvari, M. Fourmigué, *Organometallics* **2003**, *22*, 2042–2049.
[23] M. J. Begley, D. B. Sowerby, I. Haiduc, *J. Chem. Soc. Dalton Trans.* **1987**, 145–150.
[24] "The Cambridge Structural Database: A Quarter of a Million Crystal Structures and Rising": F. H. Allen, *Acta Crystallogr. Sect. A* **2002**, *B58*, 380–388.
[25] M. R. St-J. Foreman, A. F. Hill, A. J. P. White, D. J. Williams, *Organometallics* **2003**, *22*, 3831–3840.
[26] M. Bao, T. Hayashi, S. Shimada, *Dalton Trans.* **2004**, 2055–2056.
[27] a) The X-ray crystal structure of $[Bi(\kappa^3\text{-}Tm^{Me})(\kappa^1\text{-}Tm^{Me})I]\cdot 1.5\,DMF\cdot H_2O$ shows it to be crystallographically isomorphous with the corresponding antimony bromide and iodide complexes. b) The structure of $[Bi(\kappa^3\text{-}Tm^{Me})_3]NO_3\cdot 2\,DMF$ was less than ideal, with R(all data) = 0.089, $wR2 = 0.175$ and maximum residual electron density of 1.929 e Å^{-3} in the vicinity of the bismuth atom. This was the result of difficulties in performing a meaningful absorption correction, disordered solvent and a disordered nitrate (or possibly nitrite) anion. The identity of the cation is unambiguous nevertheless. Details of these structure determinations have been deposited at the Cambridge Crystallographic Data Centre (CCDC 274853 and 274854).
[28] M. Paneque, S. Sirol, M. Trujillo, E. Gutiérrez-Puebla, M. A. Monge, E. Carmona, *Angew. Chem.* **2000**, *112*, 224–227; *Angew. Chem. Int. Ed.* **2000**, *39*, 218–221.
[29] N. J. Hill, W. Levason, R. Patel, G. Reid, M. Webster, *Dalton Trans.* **2004**, 980–981.
[30] N. W. Alcock, *Adv. Inorg. Chem. Radiochem.* **1972**, *15*, 1–58.
[31] *Chemistry of Arsenic, Antimony and Bismuth* (Ed.: N. C. Norman), Thomson Science, London, **1998**.
[32] R. J. Gillespie, I. Hargittai, *The VSEPR Model of Molecular Geometry*, Allyn and Bacon, Boston, **1991**.
[33] a) P. Pykko, *Chem. Rev.* **1988**, *88*, 563–594; b) N. Kaltsoyannis, *J. Chem. Soc. Dalton Trans.* **1997**, 1–12.
[34] R. D. Hancock, J. H. Reibenspies, H. Maumela, *Inorg. Chem.* **2004**, *43*, 2981–2987.
[35] B. F. Hoskins, E. R. T. Tiekink, T. G. Winter, *Inorg. Chim. Acta* **1985**, *99*, 177–182.
[36] T. Ito, *Acta Crystallogr. Sect. E* **2004**, *60*, m783–m784.
[37] B. W. Wenclawiak, S. Uttich, H. J. Deiseroth, D. Schmitz, *Inorg. Chim. Acta* **2003**, *348*, 1–7.
[38] K. Tani, S. Hanabusa, S. Kato, S. Mutoh, S. Suzuki, M. Ishida, *J. Chem. Soc. Dalton Trans.* **2001**, 518–527.
[39] R. Hernandes-Molina, A. J. Edwards, W. Clegg, A. G. Sykes, *Inorg. Chem.* **1998**, *37*, 2989–2994.
[40] G. M. Sheldrick, SHELX97, Programs for Crystal Structure Analysis (Release 97–2), Institut fur Anorganische Chemie der Universitat Göttingen, Göttingen (Germany), **1998**.
[41] L. J. Farrugia, *J. Appl. Crystallogr.* **1999**, *32*, 837–838.

Received: June 13, 2005